Visualization of Minute Mechanical-Excitation/Relaxation Wave-front Propagation in Myocardial Tissue

Hiroshi Kanai[†] and Motonao Tanaka[††]

[†]Departments of Biomedical Engineering and Electronic Engineering,
Tohoku University, 6-6-05 Aramaki-aza-Aoba, Sendai 980-8579, Japan

[††]Cardiovascular Center, Tohoku Welfare Pension Hospital,
1-12-1 Fukumuro, Miyagino-ku, Sendai 983-0005, Japan

[†]e-mail: kanai@ecei.tohoku.ac.jp

Unlike the case of skeletal muscle, the direction of myocardial contraction does not coincide with the direction of work necessary to eject the intraventricular blood, contributing to great complexity of the wall deformation sequence of cardiac contraction. The advent of advanced techniques (CT[1], MRI[2,3], SPECT[4], echocardiology[5-9], electrocardiography[10], and magnetocardiography[11,12]) has enabled to the evaluation of cardiac function and disorders by the measurement of blood flow, pressure, electrical reaction process, and other factors. However, *complexity of the contraction sequence* is still not fully understood because the dynamic *mechanical excitation* process, which directly correlates with contraction, cannot be accurately measured based on these electro-magnetic phenomena. Here, developing and using a noninvasive novel imaging modality with high temporal and spatial resolutions[13-17], we show that the propagation of the mechanical wave-front occurs at the beginning of each cardiac contraction and relaxation sequence for the first time. The former occurs about 60 ms prior to the ordinarily accepted onset time of the contraction (R-wave of the electrocardiogram). From the apical side of the interventricular septum, close to the terminal of the Purkinje fibers (specialized to carry contraction impulses), a minute velocity component with an amplitude of several tenth micrometers is generated and propagates sequentially to the entire left ventricle, that is, it propagates from the apex to

the base of the posterior wall, and then from the base to the apex of the septum, with a propagation speed of 3-9 m/s. The latter occurs at the end of the first heart sound at the apical side and propagates to the base side with a speed of 0.6 m/s. These physiological findings, unlike the widely accepted myocardial excitation process, have potential for accurate assessment of myocardial tissue damage in coronary disease and cardiomyopathy. This dynamic measurement modality is also applicable to various tissues in biology.

TEXT Over seven million people in the world die annually from ischemic heart disease[18], the top cause of mortality. Based on the fact that polarization of cells does not occur in an infracted myocardium resulting from coronary artery occlusion[19], electrocardiography is an invaluable clinical tool for the diagnosis of cardiac failure.

By using 660 electric terminals, the time course of the excitation process has been identified[20], but only for isolated human hearts. Electrocardiographic measurement[10] has realized noninvasive imaging of the spatial distribution of action potentials, and magnetocardiography[11,12] conducted inside a shielded room enables similar imaging. These approaches should solve the inverse problem from a huge number of measurements on the chest wall regarding electric or magnetic activities. Moreover, *mechanical properties* of myocardial velocity and contraction have not been measured.

Other cardiac imaging tools, namely, CT[1], MRI[2,3], SPECT[4], and conventional echocardiography[5-7], enable visualization of 2D or 3D images, motion, torsional deformation during contraction, asynchronous wall motion during acute myocardial ischemia[21], and propagation velocity of the left ventricular inflow[22]. The time of peak contraction of the heart wall has been reported using 3D MRI tagging[23] with a temporal resolution of 35 ms. With MRI tagging, the onset time of the contraction has been reported in animal experiments[24] and human subjects[25,26]. However, their visualization is restricted to static configurations or *large* and *slow* motion due to contraction. Using the Doppler effect of the ultrasound, the instantaneous velocity or displacement are measured[8,9], but an accurate waveform for which the frequency analysis is applicable is not obtained, and measurement of minute, rapid velocity waveforms at the beginning of the contraction in the heart wall has not been attempted.

We have previously found that the rapid response of the excised heart muscle of a rat is minute (displacement of 30 μm and velocity of 0.5 mm/s)[27] and that *velocity measurement* is superior to *displacement measurement* since the displacement is the

accumulation of velocity, that is, low-pass filtering[13].

To realize *noninvasive* detection of such minute mechanical responses to the propagation of the action potential in the human heart, a novel ultrasound-based noninvasive method[16] was applied to human subjects, and we successfully measured such response as a velocity waveform for the first time[17]. In the present study, the regional change in length or wall thickness was also simultaneously measured with high temporal resolution to confirm whether the detected velocity component corresponds to the myocardial contraction or extension. Wall motion (velocity waveform) and the change in regional length (contraction/relaxation) are not a direct measurement of electrical activation, but one of the best surrogates for representing the myocardial response to excitation.

In *in vivo* experiments, by applying this novel method to the longitudinally sectional plane of a healthy human heart as shown in **Fig. 1a**, the velocity signal was transcutaneously measured as a waveform at each point on the plane. The velocity waveforms measured at six points (a-j) in **Fig. 1a** and their integration, the displacement waveform, are shown in **Figs. 1d and 1c**, respectively, for one cardiac cycle. The well-known LV contraction during the ejection period is roughly shown in the upward displacement (to inferior) of **Fig. 1c**. In the velocity waveform of **Fig. 1c**, from the time of the P-wave, T_P, of the electrocardiography, there is downward velocity component (to superior), corresponding to the expansion of the left ventricle (LV) due to atrial contraction. After this, during systole, the upward velocity component (to inferior) begins, which corresponds to the LV contraction, continuing until the time of the second heart sound, T_{II}, the time of the aortic valve closure, which is followed by rapid filling and slow filling phases, where these points moves downward (to superior).

As shown in **Fig. 1c**, however, there are some differences among these transient times from downward to upward or from upward to downward at the base-side points (d

or i). To clearly show these time differences in transition regardless of the minuteness of the velocity, by applying the moving short-time Fourier transform to each of the velocity waveforms, simultaneously measured at all points set along the lines (a-b-c-d-e, g-f, and a-j-i-h) in **Fig. 1a**, the phase of the 40-Hz component is color-coded, and its temporal change is shown in **Fig. 1b**. Red shows the upward velocity component toward the probe (point O) in **Fig. 1a**, and light blue shows its reverse property. As shown in **Fig. 1b**, the onset time of the upward velocity (contraction) before T_R does not coincide at all points (a-j), but there are some propagating components in the LV.

By expanding the time axis in **Figs. 1b and 1d**, the transition properties around T_R are shown in **Figs. 2a and 2c**, respectively. At the same time, the instantaneous change in length (shortening due to contraction or extension) is obtained at the points (a, c, j) shown in **Fig. 2b**. The white dotted lines in **Fig. 2a** show the onset of the contraction determined by confirming whether the red component of velocity is associated with the change in length from extension to contraction as in **Fig. 2b**. The black dotted lines show the reverse phenomenon.

From T_P, the atrial contraction begins and the LV volume increases, corresponding to the downward velocity (light green) in **Fig. 2a** to show the extension both in the posterior wall (b-c-d) and the interventricular septum (IVS) (a-j-i). Then, from the time 80 ms prior to T_R, the upward velocity component is generated at the apical side (a), and then from the time of 50 ms prior to T_R, the upward component propagates from the apex (b) to the base (e) along the LV posterior wall with a speed of about 9 m/s, as shown in **Fig. 2a**, where it is accompanied by the transition from extension to contraction as shown in **Fig. 2b**. It then propagates along the IVS from point (i) to both the apex (a) and the base (h) at a speed of about 3 m/s. Just after passage of this component, the contraction begins at each point. The starting point (a) of the velocity component accompanying the contraction in **Fig. 2a** would be close to

the terminal of the Purkinje fibers (special electrical conducting cells which rapidly transmit an electrical excitation)[19]. For example, at point (c), the upward velocity of 2 mm/s, which corresponds to 60 μm in displacement during 30 ms, and the contraction speed of 0.1 (m/s)/s, which corresponds to 3 μm in contraction of the 1 mm-length region, are too minute to be identified by other methods.

The first heart sound following the QRS-complex is traditionally thought to be primarily associated with mechanical vibrations resulting from the closure of the mitral values and the opening of the aortic valve[28]. As shown in **Fig. 2a**, after T_R, two waves are generated and propagate from the apex (a) to the base (e) along the LV posterior wall.

During the short period of 20 ms from the beginning of the first heart sound, the contraction property, which begins at the above onset in **Fig. 2a**, is reversed. This cessation of the contraction would correspond to the LV expansion in the pre-ejection period that is necessary to cause the mitral valve closure[29]. This cessation is terminated by the beginning of the second component of the above two waves in **Fig. 2a**, and after this cessation, all the points have the upward velocity components (red in **Fig. 2a**), that is, the contraction restarts, which constitutes the substantial LV contraction in the ejection period.

From the end of the first heart sound, the propagation of another mechanical wave-front is shown by a black dotted line in **Fig. 2a**, that is, the downward velocity component with extension occurs at the apical side and propagates to the LV base side with a speed of 0.6 m/s.

For the same subject, the position and the direction of the ultrasonic probe are changed so that the velocity and change in thickness are measured in the parasternal short-axis cross-sectional plane of the LV, as shown in **Fig. 3a**. **Figures 3d and 3b** respectively show the velocity waveforms at four points (a-b-c-d) in **Fig. 3a** and temporal changes in the phase of the velocity waveform for one cardiac cycle. **Figure**

3c shows the displacement waveforms at these points. Roughly, during the ejection period, the LV contraction is associated with the downward displacement (to posterior) at point (a) and upward displacement (to anterior) at points (b, c), while point (d) is almost motionless.

By expanding the time axis in **Fig. 3**, the mechanical excitation is shown in **Fig. 4** around T_R. From a time 120 ms prior to T_R, the response propagates from the IVS (a), to the posterior wall (b-c-d) with a speed of about 6 m/s in the counterclockwise direction when viewed from the inferior. The propagation is unidirectional, that is, the contraction propagates in one direction (counterclockwise), not in both directions. The passage of the component (blue in **Fig. 4a**) is accompanied by thickening (at a and c) or contraction (at b and d) along the ultrasonic beam; both correspond to the contraction.

Previous studies have defined the pre-ejection period[29,30] as the interval from the onset of the QRS-complex to the time of the aortic valve opening. The end of the cessation in **Figs. 2a and 4a** corresponds to the traditionally accepted onset time of the contraction[25,26]. However, the minute contraction propagation occurring prior to the onset time was found in the present study.

Similar results were obtained for other young healthy subjects. The results along the line (a-j-i) passing through the IVS from the time of the Q-wave to T_R in the top of **Fig. 2a** correspond to those in previously reported studies[17,31,32] and the cessation of the contraction has also been shown in previous studies[31,32].

It has been suggested that the myocardium is a single muscular band that conforms a double-loop helicoid[33] and that the electrical activation starts from the pulmonary artery, proceeds through the descendent segment and finally reaches the ascendant segment[34]. The propagation sequence of these walls found in the present paper would have a relationship with the suggested activation sequence.

Physiologically, it is well known that the depolarized action potentials, cyclically generated at the sino-atrial node, propagate to the Purkinje fibers, which form

interweaving networks on the endocardial surface of both ventricles and transmit the impulse almost simultaneously to the ventricular endocardium. Their conduction velocity is 2.0-4.0 m/s in the normal human[20,35] and faster than 1.0 m/s in dog ventricles[36]. Around the time of the Q-wave, based on cell-to-cell connections, the action potential starts to propagate with a lower speed of 0.3-1.0 m/s in humans[35] to the entire wall from the Purkinje fiber-myocyte junctions on the IVS surface, where the Purkinje fibers are in contact with the myocardium. In the present study, however, the measured propagation velocity regarding the minute contraction is about 9 m/s, which is much faster than those electrical conduction velocities in the previous studies. These differences suggest that the measured propagation components prior to T_R would be "pre-contraction" prior to the full contraction of the ejection period.

With the novel echocardiography employed in this study, the minute-contraction/relaxation sequences of the myocardium were confirmed noninvasively. These results show great potential for thorough understanding of the principles of the cardiac contraction/relaxation mechanism, as well as for noninvasive assessment of myocardial tissue damage in early stage of cardiomyopathy and myocardial infarction since it is known that myocardial isotonic velocity for the contraction is decreased in failing hearts[37].

Method Summary In the present study, the minute propagation of the contraction/relaxation was visualized for the first time in the human as follows: The ultrasonic beams transmitted by the ultrasound probe attached to the chest wall scan the 2D plane of the heart, and the RF reflective wave for each ultrasound transmission is acquired by the same probe as in conventional echocardiography. In this novel method, however, the phase shift between the succeedingly acquired RF signals in the same direction is determined accurately at each point in the heart wall along the ultrasonic beam, and the position of each point is tracked. Thus, the minute motion at each point

is measured as a velocity waveform so that the Fourier transform is applicable[13,14]. By restricting the number of directions of transmission to maintain a high frame rate (500 Hz), the velocity waveforms are simultaneously obtained at about 3,000 points set in the heart wall on the 2D plane[15]. By applying frequency analysis to each velocity waveform[13], the phase of its 40-Hz component is detected and its instantaneous 2D distribution is reconstructed at every 2 ms, precisely revealing the minute-wave propagation in the heart wall[15] by neglecting the amplitude component. The achieved lower limit in the velocity measurement has been validated as being 0.1 mm/s[14], which corresponds to 0.2 μm in displacement during 2 ms. Since the wavelength is about 410 μm for the typical frequency (3.75 MHz), 0.2 μm corresponds to about 1/2000 of the wavelength. Such a minute velocity component superimposed on the large motion due to heartbeat cannot be noninvasively measured by any other method. At the same time, the regional change in length of thickness is accurately obtained from the spatial difference between the velocity waveform at the adjacent points (820 μm apart) with 0.5-μm accuracy[38].

ACKNOWLEDGMENTS This study was partly supported by a grant-in-aid for scientific research from the Ministry of Education, Culture, Sports, Science, and Technology of Japan (2008-2010, No. 20360181). The authors wish to thank Dr. Hideyuki Hasegawa of Tohoku University for experimental contributions. The study was approved by the review committee of the Graduate School of Engineering, Tohoku University and the healthy subjects gave informed consent.

AUTHOR CONTRIBUTIONS M. Tanaka supervised the study. H. Kanai measured the experimental data and wrote the manuscript. Both authors analyzed the data, discussed the results, and commented on the manuscript.

REFERENCES

1. Mahoney, L. T. *et al.* Measurement of right ventricular volume using cine computed tomography. *Invest. Radiol.* **22**, 451-455 (1987).
2. Axel, L. & Dougherty, L. MR imaging of motion with spatial modulation of magnetization. *Radiology*. **171**, 841-845 (1989).
3. Buchalter, M. B. *et al.* Noninvasive quantification of left ventricular rotational deformation in normal humans using magnetic resonance imaging myocardial tagging. *Circulation.* **81**, 1236-1244 (1990).
4. Wagner, A. *et al.* Contrast-enhanced MRI and routine single photon emission computed tomography (SPECT) perfusion imaging for detection of subendocardial myocardial infarcts: an imaging study. *Lancet.* **361**, 374-379 (2003).
5. Notomi, Y. *et al.* Assessment of left ventricular torsional deformation by Doppler tissue imaging: Validation study with tagged magnetic resonance imaging. *Circulation.* **111**, 1141-1147 (2005).
6. Sutherland, G. R. *et al.* Color Doppler myocardial imaging: A new technique for the assessment of myocardial function. *J. Am. Soc. Echocardiogr.* **7**, 441-458 (1994).
7. Fleming, A. D., McDicken, W. N., Sutherland, G. R. & Hoskins. P. R. Assessment of colour Doppler tissue imaging using test-phantoms. *Ultrasound Med. Biol*. **20**, 937-951 (1994).
8. Miyatake, K., et al. New method for evaluating left ventricular wall motion by color-coded tissue Doppler imaging: in vitro and in vivo studies. *J Am Coll Cardiol*. **25**, 717-724 (1995).
9. Bax, J. J., et al. Cardiac resynchronization therapy: Part 2 - issues during and after device implantation and unresolved questions. *J Am Coll Cardiol*. **46**, 2168-82

(2005).

10. Ramanathan, C., Ghanem1, R. N., Jia, P., Ryu, K. & Rudy, Y. Noninvasive electrocardiographic imaging for cardiac electrophysiology and arrhythmia, *Nat. Med*. **10**, 422-428 (2004).
11. Stratbucker, R. A., Hyde, C. M. & Wixson, S. E. The magnetocardiogram - a new approach to the fields surrounding the heart. *IEEE Trans. Bio-Med. Electronics.* **10**, 145-149 (1963).
12. Cohen, D., Edelsack, E. A. & Zimmerman, J. E. Magnetocardiograms taken inside a shielded room with a superconducting point‐contact magnetometer. *Appl Phys Lett.* **16**, 278-280 (1970).
13. Kanai, H. *et al*. Transcutaneous measurement and spectrum analysis of heart wall vibrations. *IEEE Trans. Ultrason. Ferroelectr. Freq. Control.* **43**, 791-810 (1996).
14. Kanai, H., Hasegawa, H., Chubachi, N., Koiwa, Y. & Tanaka, M. Noninvasive evaluation of local myocardial thickening and its color-coded imaging. *IEEE Trans. Ultrason. Ferroelectr. Freq. Control.* **44**, 752-768 (1997).
15. Kanai, H. & Koiwa, Y. Myocardial rapid velocity distribution. *Ultrasound Med. Biol*. **27**, 481-498 (2001).
16. Kanai, H. Propagation of spontaneously actuated pulsive vibration in human heart wall and *in vivo* viscoelasticity estimation. *IEEE Trans. Ultrason. Ferroelectr. Freq. Control.* **52**, 1931-1942 (2005).
17. Kanai, H. Propagation of vibration caused by electrical excitation in the normal human heart. *Ultrasound Med. Biol*. **35**, 936-948 (2009).
18. World Health Statistics 2008 from World Health Organization http://www.who.int/whosis/whostat/2008/
19. Netter, F. H. *A Compilation of Paintings on the Normal and Pathologic Anatomy*

and Physiology, Embryology, and Diseases of the Heart (Ciba Pharmaceutical, Summit, NJ, 1969).

20. Durrer, D., *et al*. Total excitation of the isolated human heart. *Circulation*. **41**, 899-912 (1970).
21. Pislaru, C. *et al*. Regional asynchrony during acute myocardial ischemia quantified by ultrasound strain rate imaging. *J Am Coll Cardiol*. **37**, 1141-1148 (2001).
22. Garcia, M. J., Thomas, J. D. & Klein, A. L. New Doppler echocardiographic applications for the study of diastolic function. *J Am Coll Cardiol*. **32**, 865-875 (1998).
23. Fonseca, C. G.., Oxenham, H. C., Cowan, B. R., Occleshaw, C. J. & Young, A. A. Aging alters patterns of regional nonuniformity in LV strain relaxation: a 3-D MR tissue tagging study. *Am J Physiol Heart Circ Physiol.* **285**, H621–H630 (2003).
24. Wyman, B. T., Hunter, W. C., Prinzen, F. W. & McVeigh, E. R. Effects of single- and biventricular pacing on temporal and spatial dynamics of ventricular contraction. *Am. J. Physiol. Heart Circ. Physiol*. **282**, H372-H379 (1999).
25. Zwanenburg, J. J. M. *et al.* Timing of cardiac contraction in humans mapped by high-temporal-resolution MRI tagging: early onset and late peak of shortening in lateral wall. *Am. J. Physiol. Heart Circ. Physiol.* **286**, H1872-H1880 (2004).
26. Wyman, B. T., Hunter, W. C., Prinzen, F. W. & McVeigh, E. R. Mapping propagation of mechanical activation in the paced heart with MRI tagging. *Am. J. Physiol. Heart Circ. Physiol*. **276**, 881-891 (1999).
27. Kanai, H., Katsumata, S., Honda, H., & Koiwa, Y. Measurement and analysis of vibration in the myocardium telescopic motion for novel echo-graphic diagnosis. *Acoustical Science and Technology.* **24**, 17-22 (2003).
28. Luisada, A. A. & Portaluppi, F. *The Heart Sounds: New Facts and Their Clinical Implications.* (Praeger Scientific, New York, 1982).
29. Remme, E. W., *et al*., Mechanisms of preejection and postejection velocity spikes in

left ventricular myocardium -Interaction between wall deformation and valve events-. *Circulation.* **115**, 373-380 (2008).

30. Weissler, A. M., Harris, W. S., & Schoenfeld, C. D. Systolic time intervals in heart failure in man. *Circulation*. **37**, 149-159 (1968).
31. Yoshiara, H., Hasegawa, H., Kanai, H. & Tanaka, M. Ultrasonic imaging of propagation of contraction and relaxation in the heart walls at high temporal resolution. *Jpn. J. Appl. Phys*. **46**, 4889-4896 (2007).
32. Tanaka, M. *et al*. Blood flow structure and dynamics, and ejection mechanism in the left ventricle: Analysis using echo-dynamography. *J Cardiol*. **52**, 86-101 (2008).
33. Torrent-Guasp, F., *et al*. Spatial orientation of the ventricular muscle band: Physiologic contribution and surgical implications. *J Thoracic and Cardiovascular Surgery*. **122**, 389-392 (2001).
34. Ballester-Rodes, M., *et al*. The sequence of regional ventricular motion. *European J Cardio-thoracic Surgery*. **29S** (2006) S139—S144.
35. Katz, A. M. *Physiology of the Heart* 3rd ed. (Lippincott Williams & Wilkins, Philadelphia, 2001) page 518.
36. Sano, T., Takayama, N. & Shimamoto, T. Directional difference of conduction velocity in the cardiac ventricular syncytium studied by microelectrodes. *Circ. Res.* **7**, 262-267 (1959).
37. Spann, J. F. Jr., Buccino, R. A., Sonnenblick, E. H., & Braunwald, E. Contractile state of cardiac muscle obtained from cats with experimentally produced ventricular hypertrophy and heart failure. *Circ. Res.* **21**, 341-354 (1967).
38. Kanai, H., Sugimura, K., Koiwa, Y. & Tsukahara, Y. Accuracy evaluation in ultrasonic-based measurement of microscopic change in thickness. *Electronics Letters.* **35**, 949-950 (1999).

FIGURE LEGENDS

Figure 1. Time sequence of velocity and displacement in the unfolded left ventricular wall based on the apical view.

a. Cross-sectional image from apical view of the LV of a healthy young subject. The two colored lines passing through the walls show the phase of the 40-Hz component of the velocity wave at each point at T_R. Red and light blue correspond to the upward and downward movements, respectively.

b. Temporal changes in the phase of 40-Hz component of the velocity wave for one cardiac cycle along the two lines in Fig. 1a. Vertical axis corresponds to the line in Fig. 1a.

c. Displacement waveform at 6 points (a-j) in Fig. 1a.

d. Velocity waveform at 6 points (a-j) with ECG and PCG.

(ECG = electrocardiogram; PCG = phonocardiogram (heart sound); LV = left ventricle; RV = right ventricle; LA = left atrium; IVS = interventricular septum; PW = posterior wall; Ao = aortic valve; Mv = mitral valve; T_R = time of R-wave, T_P = time of P-wave, T_{II} = time of the second heart sound).

Figure 2. Expanded version of Fig. 1 at the beginning of the contraction.

a. Temporal changes in the phase of the 40-Hz component of the velocity wave in Fig. 1b around T_R.

b. Temporal changes in thickness or length at 6 points (a-j) in Fig. 1d around T_R.

c. Velocity waveform at 6 points (a-j).

Figure 3. Time sequence of velocity and displacement in the unfolded left ventricular wall made based on the short-axis view.

a. For the same subject as in Fig. 1, short-axis cross-sectional plane on the LV with the papillary muscle level.

b. For one cardiac cycle, the temporal changes in the phase of the velocity component. Vertical axis corresponds to the colored line in Fig. 3a.

c. Displacement waveform at points a-d in Fig. 3a.

d. Velocity waveform at points a-d.

Figure 4. Expanded version of Fig. 3 at the beginning of the contraction**.**

a. Temporal changes in the phase of the velocity component in Fig. 3b for the period around T_R.

b. Typical waveforms of the change in thickness at point c and change in length at point b.

c. Velocity waveform measured at points a-d in Fig. 3d around T_R.

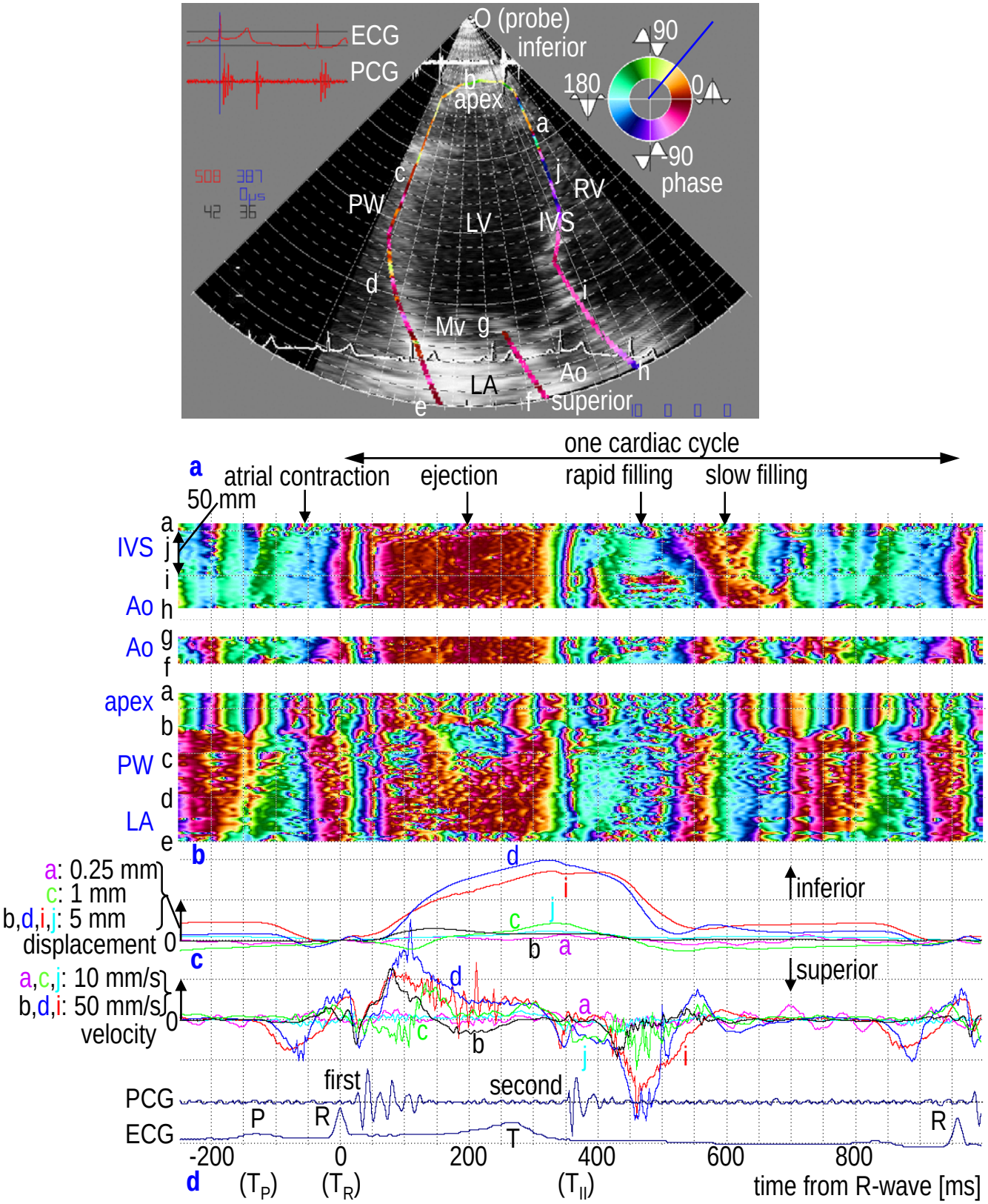
ECG
PCG
O (probe)
inferior
apex
90
180
0
-90
phase
a
j
RV
c
PW
LV
IVS
d
i
Mv
g
Ao
h
LA
e
f
superior
one cardiac cycle
atrial contraction
ejection
rapid filling
slow filling
a
50 mm
IVS
j
i
Ao
h
Ao
g
f
apex
a
b
PW
c
d
LA
e
b
a: 0.25 mm
c: 1 mm
b,d,i,j: 5 mm
displacement
0
inferior
c
a,c,j: 10 mm/s
b,d,i: 50 mm/s
velocity
0
superior
first
second
PCG
ECG
P
R
T
R
-200
0
200
400
600
800
d
(TP)
(TR)
(TII)
time from R-wave [ms]

Fig. 1

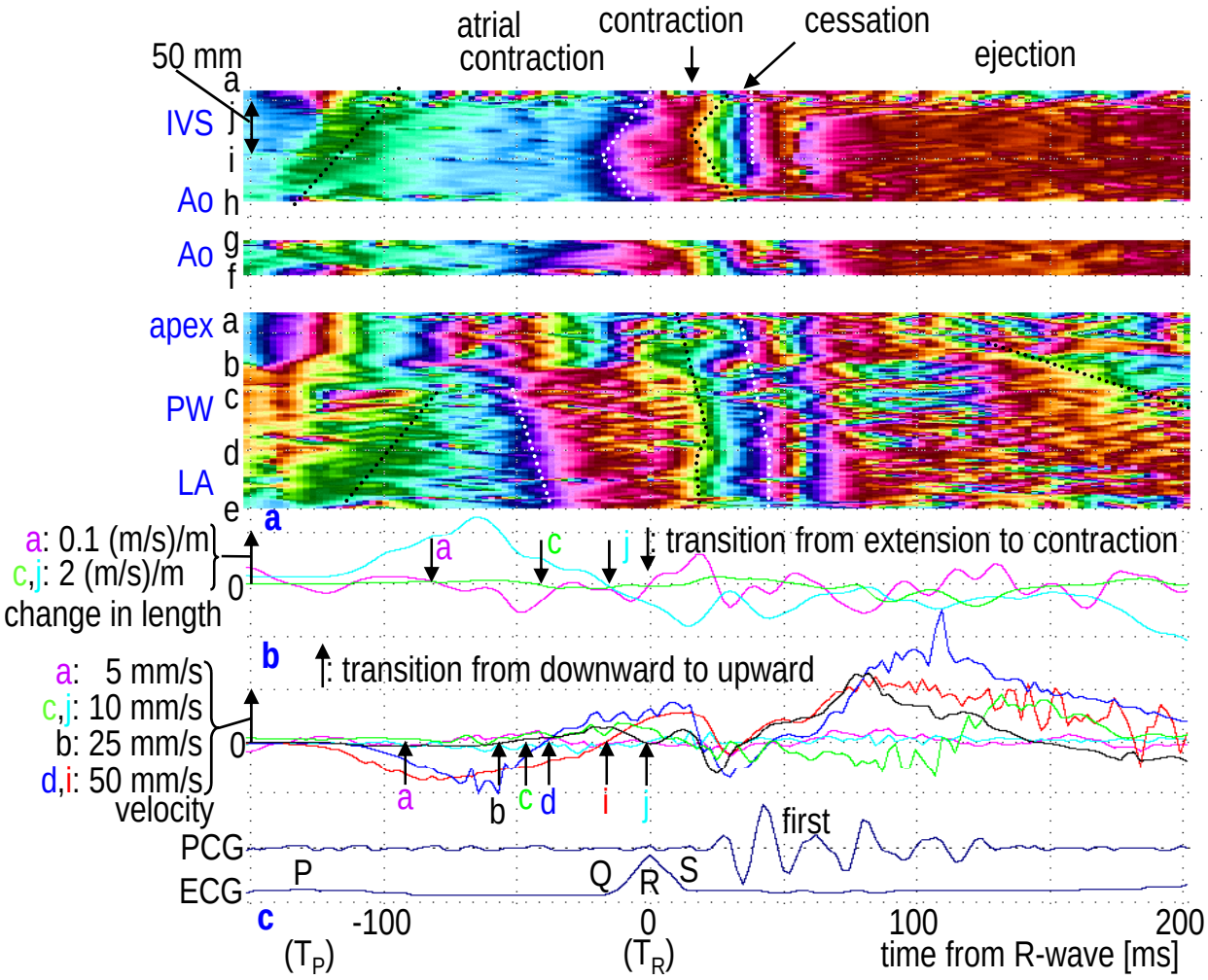
atrial contraction
contraction
cessation
ejection
50 mm
IVS
Ao
Ao
apex
PW
LA
a
b
c
d
e
f
g
h
i
j
a: 0.1 (m/s)/m
c,j: 2 (m/s)/m
change in length
: transition from extension to contraction
a: 5 mm/s
c,j: 10 mm/s
b: 25 mm/s
d,i: 50 mm/s
velocity
: transition from downward to upward
PCG
ECG
first
P
Q
R
S
-100
0
100
200
(T_P)
(T_R)
time from R-wave [ms]

Fig. 2

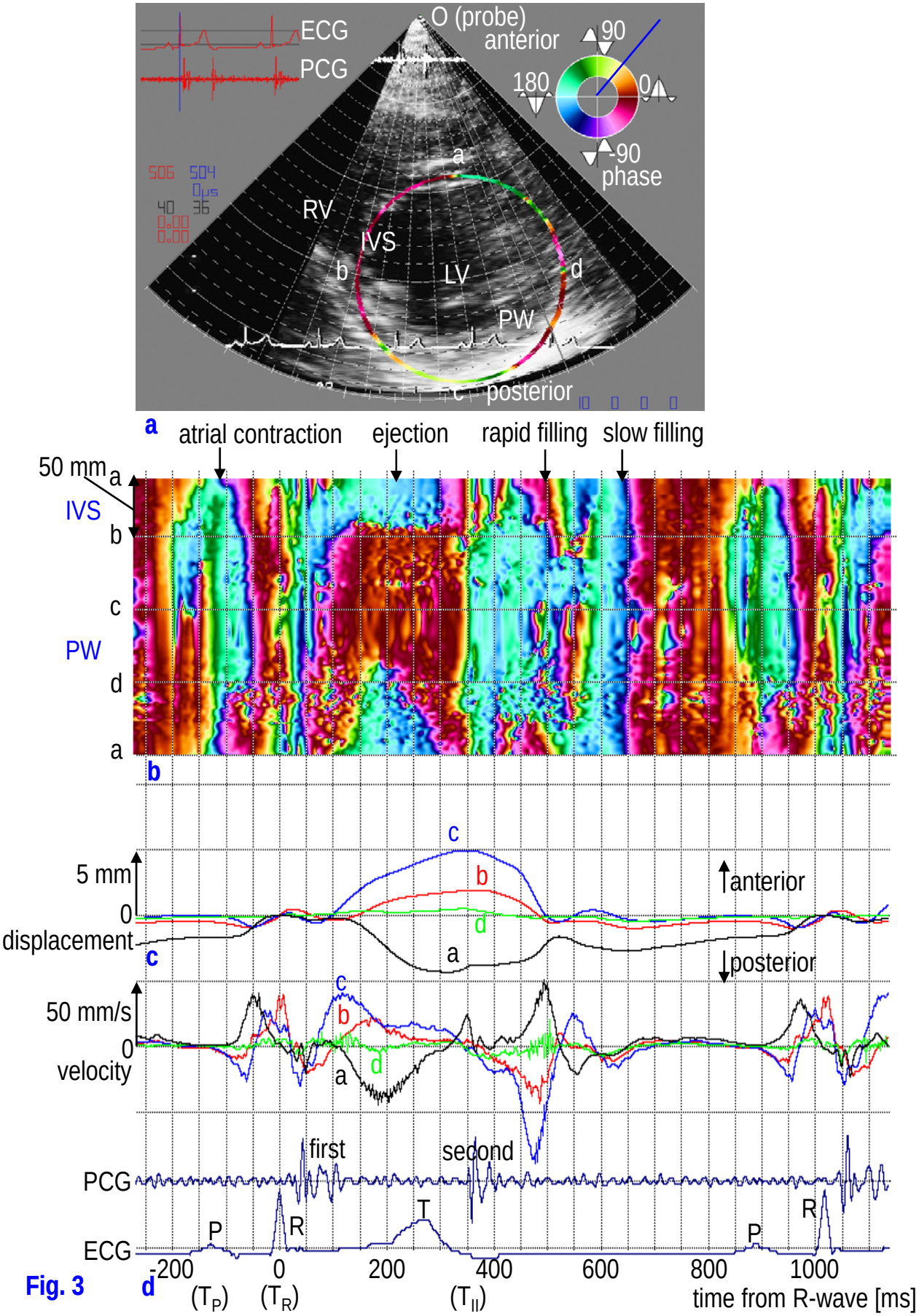
ECG
PCG
O (probe)
anterior
90
180
0
-90
phase
a
RV
IVS
b
LV
d
PW
c
posterior
a
atrial contraction
ejection
rapid filling
slow filling
50 mm
IVS
PW
b
c
5 mm
displacement
anterior
posterior
50 mm/s
velocity
first
second
PCG
ECG
P
R
T
-200
0
200
400
600
800
1000
(T_P)
(T_R)
(T_II)
time from R-wave [ms]

Fig. 3

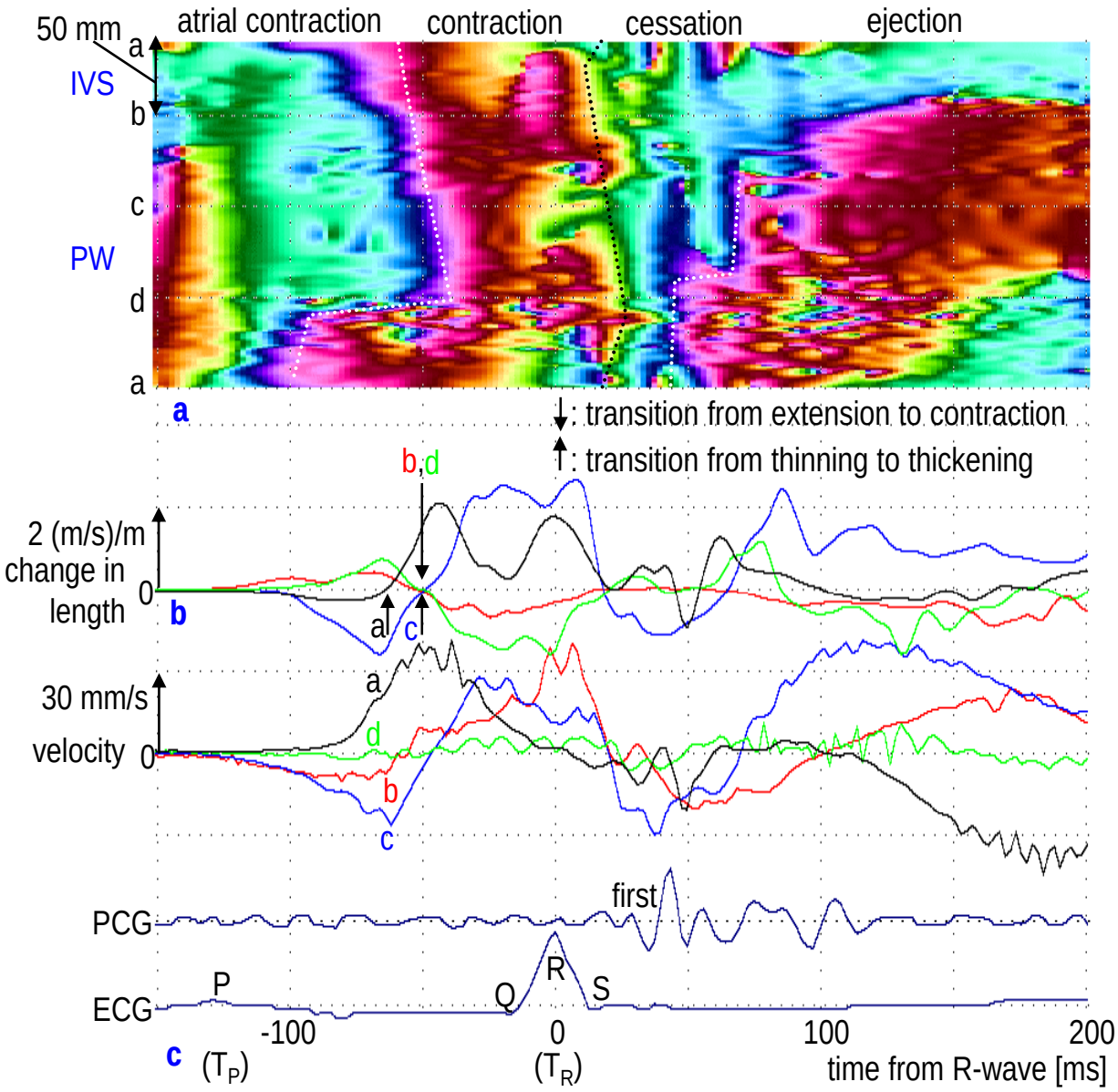
50 mm
atrial contraction
contraction
cessation
ejection
a
IVS
b
c
PW
d
a
a
: transition from extension to contraction
: transition from thinning to thickening
b,d
2 (m/s)/m
change in
length
0
b
a
c
30 mm/s
velocity
0
a
d
b
c
first
PCG
ECG
P
Q
R
S
-100
0
100
200
c
(T_P)
(T_R)
time from R-wave [ms]

Fig. 4